CILAMCE 2017
Florianópolis - Santa Catarina - Brazil

URANS SIMULATION: NUMERICAL STUDY OF FLOW AROUND A TWO DIMENSIONAL CIRCULAR CYLINDER

Fredi Cenci

André Luís Condino Fujarra

fredicenci1@gmail.com

andre.fujarra@ufsc.br

Universidade Federal de Santa Catarina

Rua Dr. João Colin, 2700, Zip-Code: 89218-035, Joinville, Santa Catarina, Brazil

Abstract. *Cylindrical geometries are frequently present in offshore structures such as monocolumns and spar oil platforms. The flow around these structures may result in complex vortex shedding systems, hence resulting in undesirable vibrations and motions known as Vortex-Induced Vibration (VIV) and Vortex-Induced Motion (VIM) phenomena. This article shows how to perform a Unsteady Reynolds-averaged Navier-Stokes (URANS) simulation of a two-dimensional fixed cylinder using OpenFOAM software as a basic approach of offshore platforms. The primary target of this paper are beginners in Computer Fluid Dynamics (CFD) modeling, thus it presents details and relevant information about the set up process as well as the verification and validation analysis. This paper gradually built a two dimensional rigid cylinder test case at subcritical region (Re = 10000), then processed 21 cases varying time-step and number of cells, following with the verification and validation procedure. The study recovered the main vortex-shedding pattern present in experiments and found secondary vortices in the near wall behind the cylinder, this last result also reported in others numerical studies. This article has shown that URANS simulation is deeply dependent of a set of computational parameters, which must be carefully investigated in order to achieve reliable results, particularly when using the OpenFOAM software.*

Keywords: *Vortex shedding, Computer fluid dynamics, Fluid structure interaction, Rigid cylinder*

1 INTRODUCTION

There is a wide range of applications for cylindrical geometries in engineering such as: buildings, cooling and water towers and offshore systems. Similarly, offshore structures such Monocolumn Production, Storage and Offloading Systems (MPSO) and spar oil platforms are geometrically similar to a finite-height cylinder and interact constantly with ocean current. This interaction may result in undesirable resonant mechanisms of oscillation known as Vortex-Induced Vibration (VIV) and Vortex-Induced Motion (VIM) phenomena.

According to Rodolfo et al. (2011) VIM and VIV are the same phenomena, however VIM is characterized in cylinders with low aspect ratios ($L/D < 4.0$) and unity mass ratio ($m^* = 1.0$, i.e. structural mass equal to the mass of water displaced). Additionally, motion amplitudes in MPSO may be as high as their characteristic diameter, reducing fatigue life of mooring and risers systems. Therefore, there is interest in understanding the flow around finite-height cylinders in order to identify interactions among vortex structures developed in these problems, determining the vortex system which arises the VIM phenomena. Palau-Salvador et al. (2009) point out that flow past long cylinders is very complex on account of highly unsteady vortex shedding. On the other hand, finite-hight cylinders mounted on wall are even more complex due to end effects where both ground and free end interact with the flow system.

Experimental investigation on VIM of offshore platforms are mostly difficult due to high costs of circulating water tanks and experimental apparatus, hence numerical solutions have been used to investigate VIM on offshore structures. Numerical solutions are commonly performed on Computer Fluid Dynamics (CFD) scheme. It offers advantages upon experiments because of flow visualization and flexibility to change parameters quickly, such as: the Reynolds number, aspect ratio and geometric details. Nonetheless, numerical studies of three dimensional geometries are often computationally expensive and time demanding for turbulent flows.

Considering all aspects exposed before, this paper aims to construct a two dimensional simulation of a smooth rigid cylinder at the subcritical region (Re = 10000). This is a very simple way to study a MPSO or spar offshore structure, analyzing the problem by its cross section. Although flow around circular smooth cylinders is a canonic problem in CFD, flow at subcritical Reynolds are hard to calculate because the flow transits to turbulent in the wake, whereas it is still laminar on the cylinder wall. According to Rosetti et al. (2012) Direct Numerical Simulations (DNS) is the only CFD method that solves all spatial and temporal turbulence scales and capable of reproducing the cylinder problem. At the same time, DNS is computationally expensive and it is normally not applicable for real engineering problems. The Large Eddies Simulations (LES) is less accurate than DNS and it has been used for high Reynolds numbers and complex geometries, considering that turbulent scales in free shear layer zones are captured. Nevertheless, near to the walls, turbulence is modeled compromising wall-bounded flows. On Unsteady Reynolds-averaged Navier-Stokes (URANS) method, all turbulence scales are averaged and not simulated. Turbulence is modeled by turbulence models, speeding up simulations.

Studies have shown that URANS eddy viscosity models cannot quantitatively reproduce experimental results in high Reynolds flow around two dimensional fixed cylinders, due to many source of errors. Even though, recognized as the most suitable method for designing platforms, the URANS numerical studies can be found for a wide range of Reynolds numbers, for instance in Rosetti et al. (2012), where the authors performed simulations based on a modern

Verification & Validation (V&V) procedure distinguishing different sources of error (numerical, modeling and experimental), simultaneously estimating numerical uncertainties. In their work, main vortex-shedding structure has been reproduced for $Re = 10000$ and secondary small vortex were developed near to cylinder associated with instabilities of the boundary layers.

Following this idea, the present work investigates URANS simulations of the flow around a fixed smooth cylinder at a subcritical Reynolds number using the free and open source software named Open source Field Operation and Manipulation (OpenFOAM), didactically conducting V&V procedure. The results are explored upon drag and lift coefficients and Strouhal number. Vortex structures are examined through flow visualization, comparing with Rosetti et al. (2012) numerical results.

2 NUMERICAL MODELING

This section presents numerical settings. Firstly problem's governing equations are identified and an appropriate turbulence model is chosen along with numerical discretization methods. Secondly, a domain is built and meshed. Then, time-step and grid size are systematically varied, creating a set of simulation cases.

2.1 Governing equations and turbulence modeling

According to Ferziger and Perić (2002), URANS approaches turbulence averaging part of the turbulence. The governing equations for incompressible flow of Newtonian fluid are the continuity and momentum equations. The averaged equations are given by Eqs. (1) and (2).

$$\frac{\partial \overline{u_i}}{\partial x_i} = 0 \tag{1}$$

$$\frac{\partial \overline{u}_i}{\partial t} + \frac{\partial}{\partial x_j}(\overline{u}_j \overline{u}_j) = -\frac{1}{\rho}\frac{\partial \overline{p}}{\partial x_i} + \frac{\partial \overline{\tau}_{ij}}{\partial x_j} \tag{2}$$

$$\overline{\tau}_{ij} = \nu\left(\frac{\partial \overline{u}_i}{\partial x_j} + \frac{\partial \overline{u}_j}{\partial x_i}\right) \tag{3}$$

Equation (3) is the mean viscous stress tensor of components. As a result of averaging the Navier-Stokes equations, the term called Reynolds stress tensor ($\tau_{ij} = -\overline{u_i^{'} u_j^{'}}$) appears and must be determined by further closure equations given by turbulence models. Because of turbulence complexity, there is not a single model capable of representing all turbulence. Most of turbulent models are based on eddy viscosity for the Reynolds stress, shown on Eq. (4).

$$-\overline{u_i^{'} u_j^{'}} = \nu_t\left(\frac{\partial \overline{u_i}}{\partial x_i} + \frac{\partial \overline{u_j}}{\partial x_j}\right) - \frac{2}{3}\delta_{ij} k, \tag{4}$$

where, ν_t is the eddy viscosity and $k = \frac{1}{2}\overline{u_i^{'} u_i^{'}}$ is the turbulent kinetic energy.

The turbulence model used in this paper is $k - \omega$ SST (Shear Stress Transport). This turbulence model uses $k - \omega$ for the inner boundary layer and $k - \epsilon$ for other regions. OpenFOAM $k - \omega$ SST model is based on Menter et al. (2003), where turbulence viscosity is obtained following Eq. (5).

$$\nu_t = a_1 \frac{k}{max(a_1\omega, F_2\mathbf{S})}, \tag{5}$$

where ω is the specific dissipation rate, $\mathbf{S}$ is the invariant measure of the strain rate and F_2 is a second blending function. For more information see Menter et al. (2003).

Values for k and ω must be determined. According to Rosetti (2015), inflow values of k and ω can be determined imposing the viscosity ratio, $f = \mu_t/\mu$, in the Eqs. (6) and (7).

$$k = 10 f \nu \frac{U_{ref}}{L_{ref}} \tag{6}$$

$$\omega = 10 \frac{U_{ref}}{L_{ref}}, \tag{7}$$

where L_{ref} and U_{ref} are reference values, whereas for the wall paths, Eqs. (8) and (9) are used.

$$k_{wall} = 0 \tag{8}$$

$$\omega_{wall} = \frac{60\nu}{0.075 y_1^2}, \tag{9}$$

in which y_1 is the first cell center height.

As shown before, terms of governing equations, such as: derivative, gradient and laplacian terms, must be discretized for numerical schemes. As the proposed problem is transient, for time derivative discretization, backward scheme is chosen. It is a transient, second order implicit and unbounded scheme. Gradient terms are discretized by linear interpolation from cell center to face, named Gauss Linear scheme, which specify gauss integration. Divergence scheme chosen is named Gauss limitedLinear α, which is linear (second order unbounded), and changes towards upwind scheme for strong gradients regions. It needs a coefficient (α), which varies from 0 to 1, where 1 means strongest limiting moving to linear as the coefficient changes to 0. Laplacian scheme selected is named Gauss linear corrected, in which "corrected" indicates explicit non-orthogonal correction. The solver selected is pisoFoam, applicable for incompressible, transient and turbulent flow using PISO algorithm.

2.2 Time and space discretization

Primarily, a computational domain must be determined. In this case, the domain's boundary must be placed far away from the interest region, thus boundaries will not affect flow over the cylinder. Computational domain has been sized based on similar simulations of previous works, such as those performed by Eça et al. (2014) and Rosetti et al. (2012). Obviously, it is interesting to keep the computational domain as small as possible because computational cost increases along with mesh size. The computational domain is shown on Fig. 1, where the frontiers are named (Inlet, Outlet, Top, Bottom and Cylinder).

Furthermore, the computational domain is meshed using blockmesh functionality, available in OpenFOAM, where mesh is constructed through a set of hexahedral blocks. Each block has number of cells and expansion ratio (relation between length of the first and last cells) in each direction. It is worth mentioning that this task can be tiring because vertices must be placed, blocks created and face defined with right orientation.

Naturally, blocks near to the cylinder have more cells and are refined in such way that non-dimensional distance y^+ is smaller than one. The condition of $y^+ < 1$ implies that cells are placed inside the viscous layer dismissing the use of wall functions. The Fig. 2 shows mesh topology near to the cylinder. To control y^+ value, functions already available in OpenFOAM must be used, for instance if the output result is $y^+ > 1$ the mesh is refined near to the cylinder's surface.

In addition to meshing, boundaries conditions must be selected for all frontiers and all variables, such as: k, ω, P, U, where P is the pressure and U is the velocity. As claimed by Rosetti et al. (2012), variables of turbulence model can be initialized by viscosity ratio f in which turbulence quantities are uniform and deduced from laminar field ($f = 0.01$). The Tab. 1 summarizes boundaries condition selected for each face.

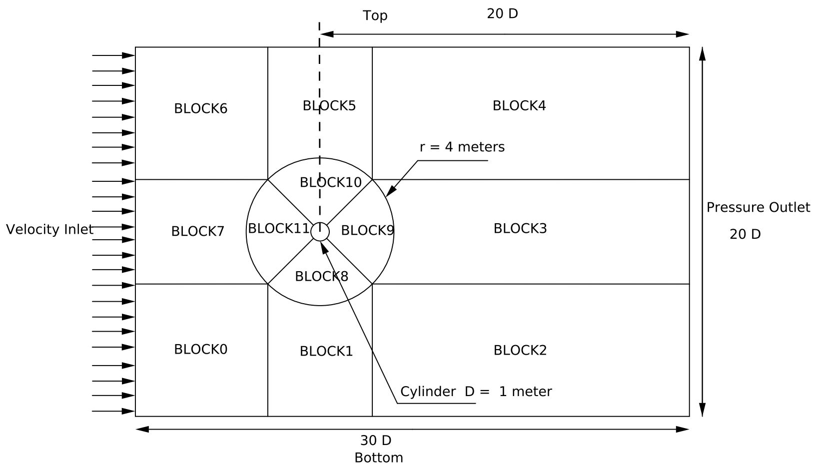

Figure 1: Computational domain.

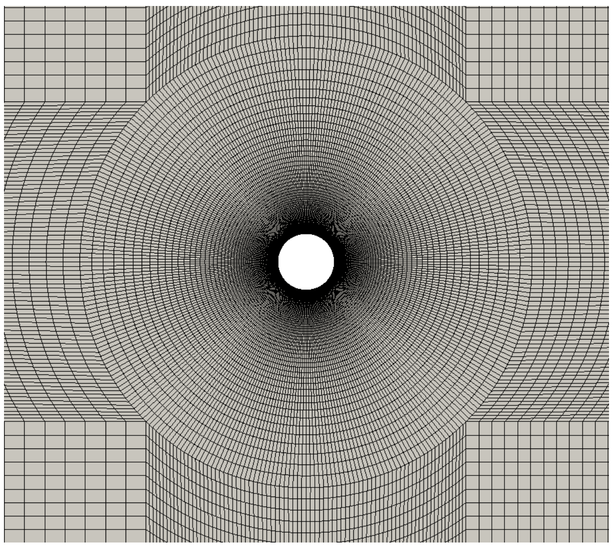

Figure 2: Mesh topology.

The condition zeroGradient means the field is completely developed and $\frac{\partial \phi}{\partial n} = 0$. Zero outlet pressure means zero static pressure. Conditions of a fixed value or zero gradient are known as Dirichlet and Newmann condition. Different of commercial softwares, which automatically select some boundary conditions, all faces must be assign a boundary condition. Select the correct boundary conditions can be a hard and tricky task in OpenFOAM for CFD beginners, therefore must be carefully investigated.

Table 1: Boundary condition for each computational domain's face.

Quantity	Face	Boundary Condition	Value
	Inlet	fixedValue	Related to Eq. (7)
ω	Outlet	zeroGradient	-
	Cylinder	fixedValue	Related to Eq. (9)
	Bottom and Top	symmetryPlane	-
	Inlet	fixedValue	Related to Eq. (6)
k	Outlet	zeroGradient	-
	Cylinder	fixedValue	Related to Eq. (8)
	Bottom and Top	symmetryPlane	-
	Inlet	fixedValue	Related to $Re = 10000$
U	Outlet	zeroGradient	-
	Cylinder	zeroGradient	-
	Bottom and Top	symmetryPlane	-
	Inlet	zeroGradient	-
P	Outlet	fixedValue	zero
	Cylinder	zeroGradient	-
	Bottom and Top	symmetryPlane	-

The last parameter to be set is solver's tolerances (tol_i). This parameter is related to iterative errors and will be discussed later on uncertainty analysis, for now the value of $tol_i = 10^{-8}$ is selected for pressure and $tol_i = 10^{-7}$ for velocity and turbulence quantities.

Finally, time-step (t) and grid size (N) were systematically varied, resulting in 21 cases. Time and space discretization is shown on Tab. 2. Not all combinations of mesh and time-step were simulated, the cases considered is shown on results section.

Table 2: Time-step and mesh characteristics

Time-step (t_i)	Value (s)	Step/Vortex cycle
t_1	0.06	551
t_2	0.04	827
t_3	0.03	1103
t_4	0.02	1654
t_5	0.01	3309
Mesh (M_i)	Number of cells (N_{cells})	Cells on cylinder surface
M_1	16600	160
M_2	46900	320
M_3	78500	400
M_4	151800	480
M_5	229500	600

3 UNCERTAINTY ANALYSIS

This section relies on Eça and Hoekstra (2009) and Rosetti et al. (2012) V&V process. Nowadays CFD simulations must conduct a Verification and Validation procedure in other to be reliable. Once the physics of a determined problem is identified, mathematical models are created to represent what is physically happening. This mathematical models are computationally implemented and must be evaluated, therefore, Verification is concern about determine if mathematical models implemented are accurate or not. On the other hand, Validation is engaged to demonstrate if a determined model is representing the reality.

Verification is divided in code verification and verification of calculation. The first attempts to verify the code itself, while the second evaluate the error of a given calculation. Thus, Verification estimates numerical error in CFD analysis. There are three main types of error: round-off error, related to computer precision; interactive error, related to non-linear equations of partial equations; and discretization error, associated with approximations such as space and time discretization.

Round-off errors may be neglected using computer's double precision. Interative error also could be neglected by using tolerances as small as computer's double precision, however this may considerably increase simulation time. In this paper double precision was used for round-off errors. Interative errors were neglected assuming tolerances of quantities (P, U, ω, k) few orders of magnitude smaller than discretization errors, as studied by Rosetti et al. (2012) and Eça et al. (2014).

The last and largest source of error, discretization error, must be analyzed. Therefore, Eq. (10) gives the discretization error estimator based on Richardson extrapolation.

$$\delta_{RE} = \phi_i - \phi_0 = \alpha_x h_i^{P_x} + \alpha_t \tau_i^{P_t}, \tag{10}$$

in which ϕ_i is the numerical solution, of a given mesh and time-step i, of an integral or scalar quantity. ϕ_0 is the exact numerical solution and must be determined. α_x and α_t are constants. h_i and τ_i are parameters which represent the grid size and time-step. P_x and P_t are space and time observed order of accuracy. Therefore, simulations must vary both, time-step and grid size solving Eq. (10) in Least-Square sense. Also, it is important to point out that this procedure implies both, round-off and interactive errors, are neglected.

For the simulations in this work, round-off error and interactive errors were neglected reducing calculation to double precision and solver's tolerance to $tol_i < 10^{-7}$. Different from Rosetti et al.(2012), residuals are controlled by L_{rms} norms instead L_∞, for that, 1 order of magnitude were decreased for the tolerances of the quantities.

This error estimator based on Richardson extrapolation depends of the convergence condition found. The options are: monotonic convergence, oscillatory convergence, monotonic divergence and oscillatory divergence.

After all simulations, the order of convergence (P) must be determined. In case of monotonic convergence is observed ($P > 0$) Richardson extrapolation can be used, else an alternative error estimator is used based on the maximum difference among the solutions simulated, as is given on Eq. (11).

$$\Delta_M = max|\phi_i - \phi_j| \text{ with } 1 > i > N_g \text{ and } 1 > j > N_g, \tag{11}$$

where N_g is the number of simulations available.

The final goal is estimate with 95% of confidence that the exaction solution is between:

$$\phi_i - U_D(\phi_i) < \phi_{exact} < \phi_i + U_D(\phi_i), \tag{12}$$

where $U_D(\phi_i)$ is the numerical uncertainty of the quantity ϕ_i.

Finally, the author gives the following conditions:

- For $0.95 \leq P < 2.05$

$$U_D(\phi) = 1.25\delta_{RE} + U_s \tag{13}$$

- For $0 < P < 0.95$

$$U_D(\phi) = min(1.25\delta_{RE} + U_s, 1.25\Delta_M) \tag{14}$$

- For $P \leq 2.05$

$$U_D(\phi) = max(1.25\delta'_{RE} + U_s, 1.25\Delta_M \tag{15}$$

- If monotonic convergence is not observed:

$$U_D(\phi) = 3\Delta_M, \tag{16}$$

where U_s is the standard deviation of the fit. δ'_{RE} is the Richardson extrapolation considering its theoretical value of $P = 2$. For more information look Eça and Hoekstra (2009).

Once the numerical uncertainty (U_D) is known, the validation analysis is conduct. For that, the final uncertainty is given on Eq. (17).

$$U_{val} = \sqrt{U_D^2 + U_E^2}, \tag{17}$$

where U_E is the experimental uncertainty, which is rare to find in publications. Experimental uncertainty was taken, assuming hypothetical infinite set of experiments and gaussian distribution, from Rosetti (2015).

4 RESULTS

As mentioned before, 21 cases with different time-steps and grid sizes were simulated. The only source of numerical error is due to discretization in space and time. Convergence analysis were conducted upon mean drag ($\overline{C}_D$) coefficient, root mean square (rms) lift coefficient (C_{Lrms}) and Strouhal number (S_t). Figures 3, 4 and 5 show characteristic curves found for C_{Lrms} and $\overline{C}_D$ coefficients and S_t number.

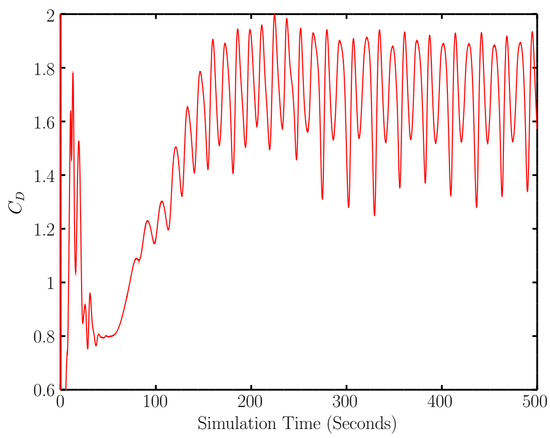

Figure 3: C_D **for** M_4 **and** t_1**.**

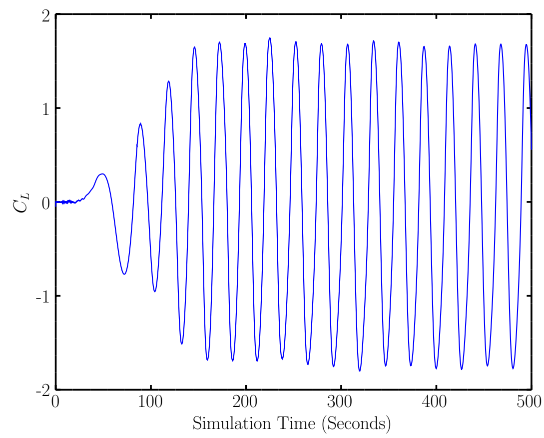

Figure 4: C_L **for** M_4 **and** t_1**.**

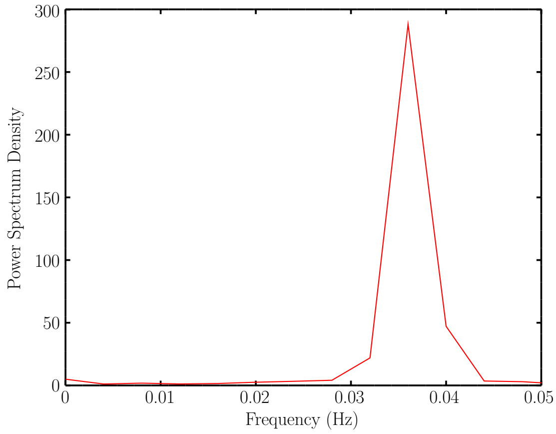

Figure 5: C_D for M_4 and t_1.

Strouhal number is obtained from a Fast Fourier Transform (FFT) applied to the lift force time histories, identifying the vortex shedding frequency (f_s) as the peak of power spectrum density graphs. This value is sensitive to number of vortex-shedding cycles, so in this work f_s is calculated considering approximately the 10-last cycles. Also, for drag and lift quantities, values before $t = 250\ s$ are discarded because it is related to transient solution, where vortex shedding is not established.

These quantities are plotted according to time-step and grid size, which are identified by Eqs. 18 and 19, where $h = 1/\sqrt{N_{cells}}$.

$$t_i/t_{min} = \Delta t/(\Delta t)_{min} \tag{18}$$

$$h_i/h_{min} = \sqrt{\frac{(N_{cells})_{max}}{(N_{cells})_i}} \tag{19}$$

Naturally, $h_i/h_{min} = 1$ represents the finest grid. In the same way, $t_i/t_{min} = 1$ the finest time-step. The coarser times, $t_i/t_1 = 6$ and $t_i/t_1 = 4$, and the coarser grid, $h_i/h_1 = 3.7$, were discarded for uncertainty analysis herein carried out in order to not contaminate the final analysis.

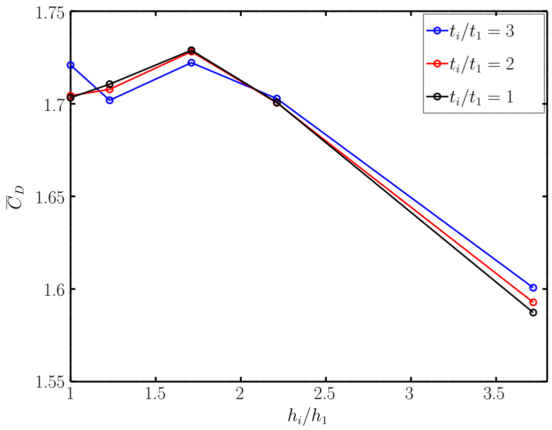

Figure 6: $\overline{C}_D$ grid discretization.

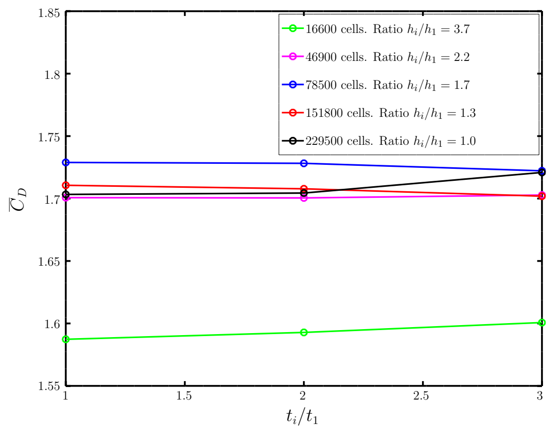

Figure 7: $\overline{C}_D$ time discretization.

Figure 7 shows that the solution is in the asymptotic region. At the same time, by inspecting Fig. 6, the variation of $\overline{C}_D$ with grid size seems not to be in the asymptotic region. Therefore, proceeding with uncertainty analysis it was found $P_t > 0$ and $P_x < 0$. Thus, as grid is not asymptotic converging, uncertainty for $\overline{C}_D$ is given by Eq. 16. The same behavior was found by Rosetti et al. (2012), in which asymptotic convergence was not observed for $Re = 10000$, indicating that this is a critical region where flow characteristics are not completely defined.

Tendency of C_{Lrms} and S_t quantities with grid and time refinement are shown on Figs. 8, 9, 10 and 11.

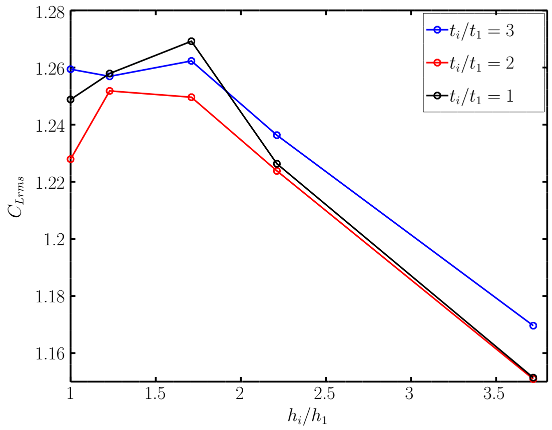

Figure 8: C_{Lrms} grid discretization.

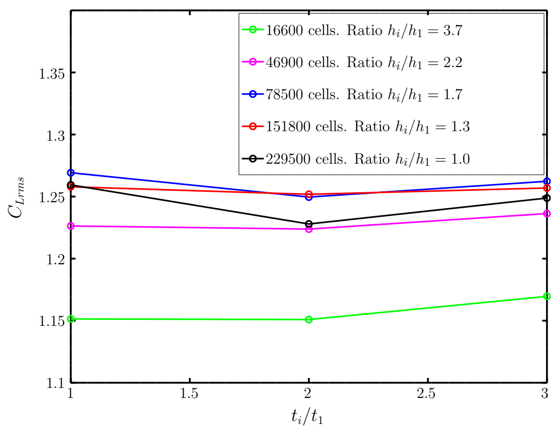

Figure 9: C_{Lrms} time discretization.

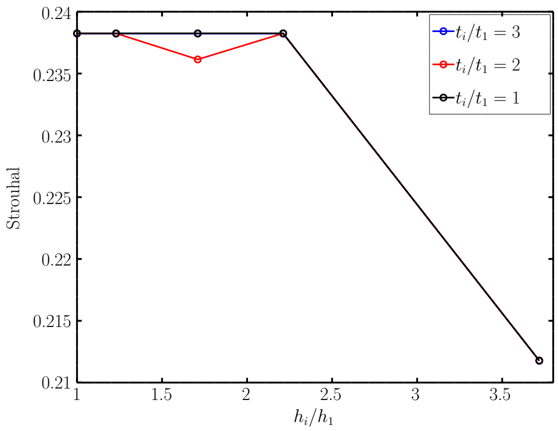

Figure 10: S_t grid discretization.

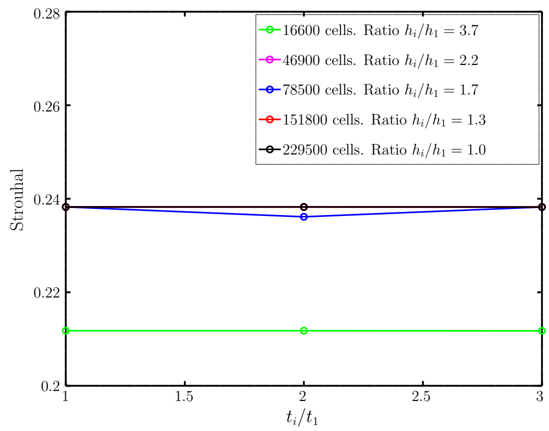

Figure 11: S_t time discretization.

Finally, after calculate all numerical uncertainty, $\overline{C}_D$, C_{Lrms} and S_t are quantitatively compared to experimental and numerical results on Figs. 13, 12 and 14.

As expected, URANS $k - \omega$ SST cannot quantitatively reproduce experimental results. Difference between experimental results and this work are 53.5% for $\overline{C}_D$, 86% for S_t and 132% for C_{Lrms}. Graphically looking at those differences, uncertainties calculated do not explain such high error, therefore it is on account of modeling errors from $k - \omega$ SST turbulence model, which overestimate the integral quantities analyzed. Furthermore, two dimensional sim-

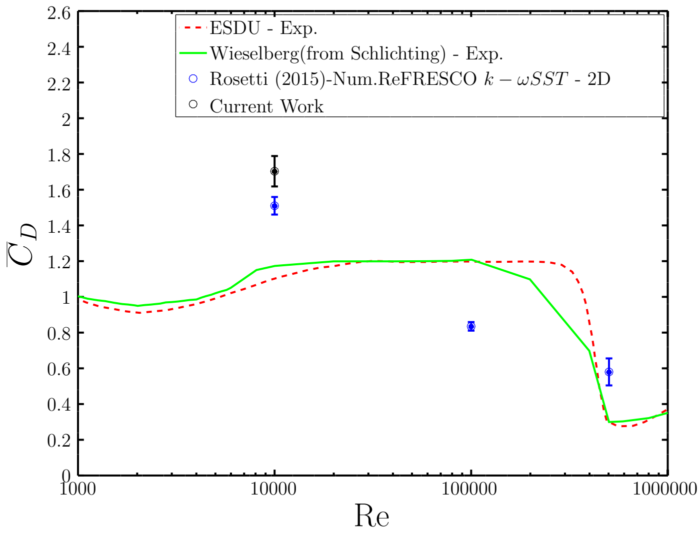

Figure 12: $\overline{C}_D$ results. Numerical results from Rosetti (2015). Experimental results from Schlichting and Gersten (2017), and ESDU (1985).

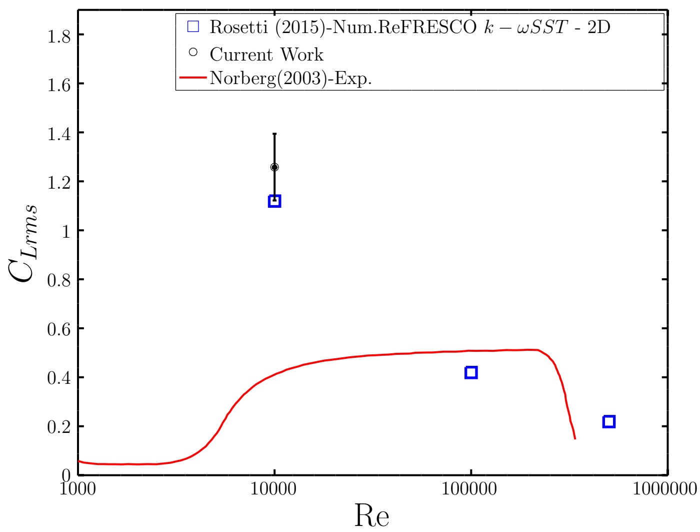

Figure 13: C_{Lrms} results. Numerical results from Rosetti (2015). Experimental results from Norberg (2003).

plification of the problem, which in fact is three dimensional, may have a considerable share of numerical/experimental divergence.

It is worth mentioning that coarser grids and time-steps outcome better results compared to experimental data. However, these results are computationally wrong and cannot be trusted. It supports the idea that V&V analysis are essential in CFD studies and design purposes.

Comparing numerical results from Rosetti (2015) using ReFresco and current work with OpenFOAM, better agreement was found between quantities. Uncertainties overlap themselves for S_t and C_{Lrms}. The same is not observed for $\overline{C}_D$, however they are considerably closer compared to experimental results. These slight differences may be on account of finer meshes

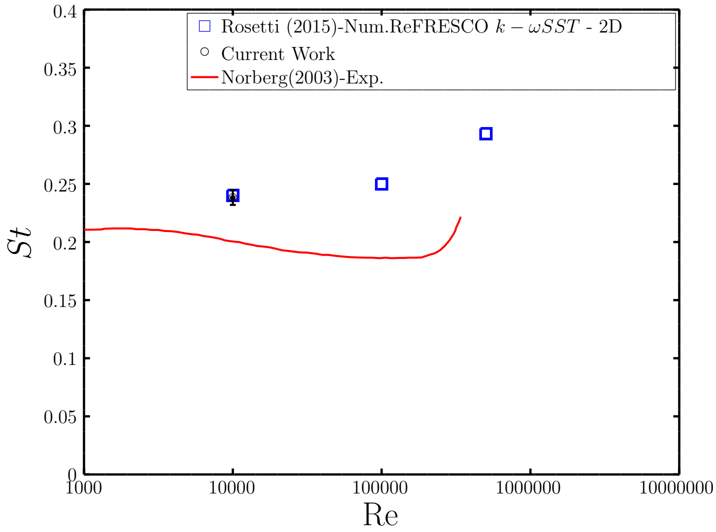

Figure 14: Strouhal number results. Numerical results from Rosetti (2015). Experimental results from Norberg (2003).

simulated and the solver SIMPLE used by Rosetti (2015), compared to the present work, which used PISO algorithm.

Proceeding with validation process for $\overline{C}_D$, total uncertainty (U_{val}) is compared with difference between numerical and experimental value ($|E|$). Experimental uncertainty was taken from Rosetti (2015) as mentioned before, therefore $U_E = 0.11$. Because $|E| > U_{val}$ the model cannot be validated.

Furthermore, flow visualization may be analyzed plotting normalized vorticity field and streamlines as shown on Figs. 15 and 16.

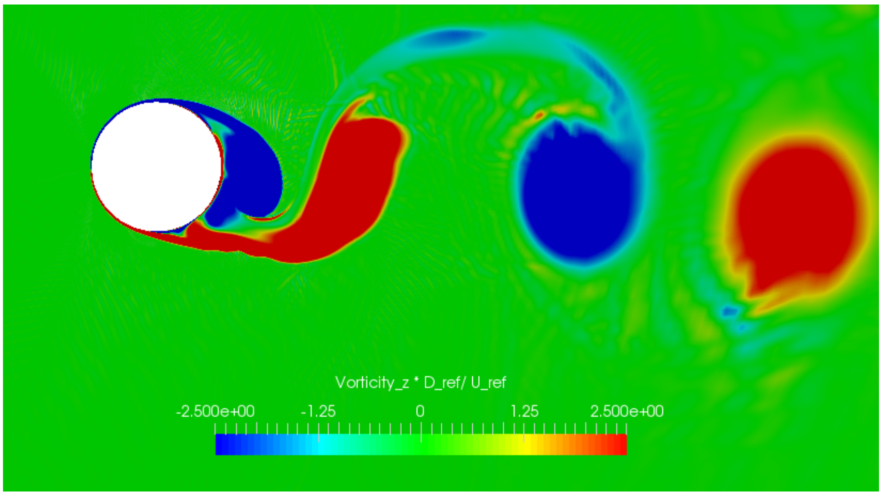

Figure 15: Normalized vorticity ($\omega_z D_{ref}/U_{ref}$), $Re = 10000$.

Characteristics of the flow around fixed cylinders were recovered. Clearly the main vortex shedding structures are formed. Also, near to the shear layers secondary vortices are developed due to instabilities as described by Rosetti et al. (2012). It was observed that these small

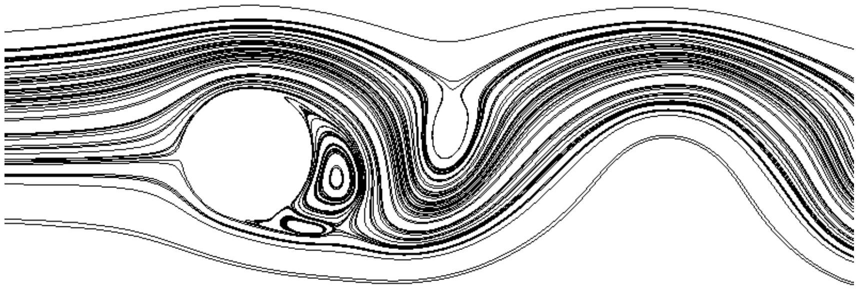

Figure 16: Streamlines plots, $Re = 10000$.

vortices eventually merge to the main vortex structures. Despite of being not possible to numerically validate the results obtained, the case herein studied with OpenFOAM agrees with those performed by means of ReFresco, recovering qualitatively vortex structures found by Rosetti et al. (2012).

5 CONCLUSION

This article didactically proceed URANS simulations of flow around a smooth fixed cylinder at $Re = 10000$ using a free and open source software OpenFOAM. It was exposed that simulation are dependent of numerous parameters and approximations. Hence, estimation of turbulence quantities, computational domain size, boundary conditions and numerical schemes must be carefully investigated in order to computationally represent the real phenomenon.

In fact, many sources of error were exposed and a V&V modern procedure conducted, indicating how to deal with numerical error sources and validate with experimental data. The procedure showed that, although coarse grids and time-steps might outcome “better” results, they are computationally wrong. Therefore, CFD simulations must carry out under verification and validation procedures in order to be reliable.

The case studied selected for this work has shown that OpenFOAM is able to reproduce vortex-shedding over cylinders. Also, secondary eddies were reproduced and asymptotic convergence not observed as found by Rosetti et al. (2012) using the software ReFresco. Additionally, although some quantities could not be quantitatively validated with experimental results due modeling errors, for engineering applications the turbulence model $k - \omega\ SST$ seems to give qualitatively satisfactory results. However, more cases must be investigated with different Reynolds numbers, what is part of a ongoing research and it will be published soon. Furthermore, three dimensional modeling investigation may reduce quantitatively divergences between numerical and experimental integrals quantities.

Finally, future works may use OpenFOAM to calculate flow around smooth cylinders with 1 and 2 degree of freedom conducting modern V&V procedure.

ACKNOWLEDGEMENTS

Fujarra acknowledges CNPq (National Council for Scientific and Technological Development, Brazil) for the financial support, grant 304600/2016-4.

REFERENCES

ESDU, 1985. *Circular Cylindrical Structures: Dynamic Response to Vortex Shedding, Part 1: Calculation Procedures and Derivation*. Regent Street, London W1R 7AD, UK, pp. 251-259.

Eça, L., & Hoekstra, M., 2009. Evaluation of numerical error estimation based on grid refinement studies with the method of the manufactured solutions. *Computers & Fluids*, vol. 38, n. 8, pp. 1580-1591.

Ferziger, J., and Peric, M., 2002. *Computational Methods for Fluid Dynamics*, 3 rd ed. Springer-Verlag.

Gonçalves, R. T., Freire, C. M., Rosetti, G. F., Franzini, G. R., Fujarra, A. L., & Meneghini, J. R., 2011. Experimental Comparisons to Assure the Similarity Between VIM (Vortex-Induced Motion) and VIV (Vortex-Induced Vibration) Phenomena. *elastic*, vol. 1, pp. 2-56.

Menter, F. R., Kuntz, M., & Langtry, R., 2003. Ten years of industrial experience with the SST turbulence model. *Turbulence, heat and mass transfer*, vol. 4 , n. 1, pp. 625-632.

Norberg, C., 2003. Fluctuating lift on a circular cylinder: review and new measurements. *Journal of Fluids and Structures*, vol. 17, n. 1, pp. 57-96.

Palau-Salvador, G., Stoesser, T., Frhlich, J., Kappler, M., & Rodi, W., 2010. Large eddy simulations and experiments of flow around finite-height cylinders.*Flow, turbulence and combustion*, vol. 84, n. 2, pp. 239-275.

Rosseti, G.F., 2015. *Improvements in the Numerical Modeling of Turbulence and Fluid-Structure Iteration for Vortex-Induced Vibrations of a Rigid Cylinder*. PhD thesis, University of São Paulo.

Rosetti, G.F., Vaz, G., Fujarra, A.L.C., 2012. URANS calculation for smooth circular cylinder flow in a wide range of Reynolds Numbers: solution verification and validation. *ASME Journal of Fluids Engineering*, vol. 134, n. 12, pp. 121103.

Schlichting, H., & Gersten, K., 2017. *Boundary Layer Theory*, 9 th ed. Springer-Verlag.